JP2.15 PROTOTYPING SST RETRIEVALS FROM GOES-R ABI WITH MSG SEVIRI DATA

N. Shabanov*[1,2], A. Ignatov[1], B. Petrenko[1,2], Y. Kihai[4], X. Liang[3], W. Guo[1,2], F. Xu[3], P. Dash[3], M. Goldberg[1], J. Sapper[5]

[1]NOAA/NESDIS, Center for Satellite Applications and Research (STAR), Camp Springs, MD
[2]IMSG Inc., Kensington, MD
[3]Cooperative Institute for Research in the Atmospheres (CIRA), Fort Collins, CO
[4]Perot Systems Government Services, Lanham, MD
[5]*NOAA/NESDIS/OSDPD*

1. INTRODUCTION

Geostationary Operational Environmental Satellite-R Series (GOES-R) with the Advanced Baseline Imager (ABI) onboard is a key future component of the NOAA program for environmental monitoring. A Sea Surface Temperature (SST) algorithm for ABI is being developed by the SST Application Team, as a part of the GOES-R Algorithm Working Group (AWG). ABI SST production is prototyped with currently available Meteosat Second Generation (MSG) Spinning Enhanced Visible and IR Imager (SEVIRI) data (Schmetz et al., 2002). The Advanced Clear-Sky Processor for Oceans (ACSPO) developed at NOAA/NESDIS and currently operational with AVHRR data onboard NOAA-18 and MetOp-A has been adapted to SEVIRI. The ACSPO-SEVIRI system processes 15-minute full-disk (FD) SEVIRI Level 1 data in near-real time (NRT) and generates a suite of Level 2 clear-sky products over ocean, including top-of-atmosphere (TOA) clear-sky Brightness Temperatures (BTs), SSTs and Aerosol Optical Depths (AOD). This paper provides a brief description and an initial assessment of the ACSPO-SEVIRI retrievals.

2. DATA

Time series of ACSPO-SEVIRI retrievals for the month of June 2008 were analyzed in this study. Meteosat-9 (MSG-2) SEVIRI 15-minute Full Disk (FD) data is the primary system input. FD data corresponds to a 3712x3712 pixel image, with 4.8 km resolution at nadir. The “SATELLITE” projection is used with the sensor positioned at (0.0;0.0) Lat/Lon position. Table 1 shows a list of SEVIRI channels used as input to the ACSPO-SEVIRI system.

Channel	Wavelength
Channel 1 (VIS)	0.635/ [0.56-0.71] µm
Channel 2 (VIS)	0.810/ [0.74-0.88] µm
Channel 3 (VIS)	1.640/ [1.50-1.78] µm
Channel 4 (IR)	3.920/ [3.48-4.36] µm
Channel 9 (IR)	10.80/ [9.80-11.80] µm
Channel 10 (IR)	12.00/ [11.00-13.00] µm

Table 1: SEVIRI channels, input to ACSPO-SEVIRI.

Two major ancillary data sources are utilized by the ACSPO-SEVIRI system: global weekly 1° fields of Reynolds SST (Reynolds et al., 2002) (soon to be replaced with the daily product, Reynolds et al., 2007), and the National Centers for Environmental Prediction Global Forecast System (NCEP/GFS) 1° 6 hour upper air data.

Multiple global reference SST fields are also appended downstream and used for quality control of the retrieved SEVIRI SST product, including OISST (Optimal Interpolation or Reynolds SST, AVHRR-based), OISST(A) (OISST with microwave AMSR-E data), RTG HR/LR (Real Time Global High/Low Resolution), OSTIA (Operational SST & Sea Ice Analysis) [cf. Table 2; for more details on the reference fields, see Dash et al., 2009].

Data Set	Resolution	Reference
OISST	1º, weekly	FTP1
OISST(A)	0.25º, daily	FTP2
RTG LR	0.50º, daily	FTP3
RTG HR	1/12º, daily	FTP4
OSTIA	0.05º, daily	FTP5

Table 2. Global Reference SST Fields used to quality control SST produced by ACSPO-SEVIRI.

3. ACSPO-SEVIRI SYSTEM

A flow-chart of the current ACSPO-SEVIRI system is shown in Fig.1. The system ingests dynamic SEVIRI FD channel data (Table 1), and dynamic FD illumination geometry data (solar zenith and relative azimuth angles). Additionally, several static FD data are required, including Land/Water Mask, View Geometry and Lat/Lon. Ancillary coarse-resolution NCEP/GFS data are used as input to the fast Community Radiative Transfer Model (CRTM) to simulate clear-sky BTs in Ch4, 9, and 10 (Liang et al., 2009). CRTM BTs are used for cloud masking, physical SST retrievals, and to monitor the quality of SEVIRI radiances. The course-resolution reference SST fields and BTs simulated by CRTM on GFS 1° grid are bi-linearly interpolated to each SEVIRI pixel.

Two SST algorithms have been implemented side-by-side in the ACSPO-SEVIRI system. The Regression (split-window, NLSST) algorithm is based on Walton et al. (1998) equation:

$$T_S=a_0+a_1T_9+a_2T_{ref}(T_9-T_{10})+a_3(T_9-T_{10})(\sec\theta-1).$$

Here, T_9 and T_{10} are BTs in SEVIRI Ch9 and 10 and T_{Ref} is the First Guess SST (currently, weekly OISST, cf. Table 2), θ is the satellite view zenith Angle, and a_0–a_3 are regression coefficients. Presently, regression coefficients derived by Meteo-France for Meteosat-8 are utilized (Le Borgne et al., 2006). The Physical algorithm uses CRTM to invert T_9 and T_{10} for SST and water-vapor optical depth scaling factor using an algorithm similar to the one described in (Merchant et al., 2008). Both algorithms have been bias-corrected using one full day of Meteosat-8 data from 28 March 2008, to approximately match Reynolds weekly SST.

Both Regression and Physical algorithm allow extension to the three-channel retrievals (Ch4, 9, and 10), Presently inclusion of Ch4 is pending resolving a substantial discrepancy of SEVIRI BTs with CRTM simulations in this band (cf. Section 4.2). Also, improvements in CRTM are underway to model solar contamination in this band during daytime. The regression and physical SST algorithms will be extensively cross-evaluated, and potentially merged into a single hybrid SST algorithm. The hybrid algorithm would combine the flexibility of accounting for local atmospheric transmission variations offered by the inversion method with a potential adjustment of some retrieval algorithm parameters against *in-situ* data, utilized in the regression methodology.

Aerosol Optical Depths (AODs) are retrieved from optical channels (Ch1-3) using single-channel LUTs (De Paepe et al., 2008). The LUTs are sensor-specific, separate LUTs were developed for two SEVIRI sensors onboard Metosat-8 (MSG1) and -9 (MSG2). In the ACSPO system, AODs are used as an additional quality indicator of the cloud mask and retrieved SSTs.

The current version of the SEVIRI cloud mask algorithm is based on ACSPO-AVHRR v.1 algorithm (Peternko et al., 2008) adjusted to SEVIRI. For this study, a simplified version of this algorithm was implemented which uses only two tests: SST test (comparison of retrieved and Reference OISST field) and BT test (comparison of CRTM simulated and measured BTs). The current Cloud Mask algorithm generates a 4-state pixel cloud flag: “clear”, “probably clear”, “cloudy”, and “invalid”, based on the outputs of the individual cloud tests. Pixel information is finally aggregated into a “pixel state byte” which contains individual cloud test bits and overall cloud flag, land/sea mask, day/night time flag, and glint flag.

Note that an updated cloud masking algorithm is currently being tested for ACSPO-AVHRR v.1.10 (Petrenko et al., 2009). Pending successful testing with AVHRR, this algorithm will be then implemented with SEVIRI. The new cloud screening approach includes a two-step process. The ACSPO Cloud Mask (ACM) is run first, which uses climatological information and fixed thresholds, followed by the ACSPO Quality Control (AQC), which fully utilizes the advantages of the more accurate first-guess SST and GFS fields used in conjunction with CRTM. Adjustments and fine tuning of the ACM and AQC will be needed.

The end-to-end NRT processing system is being set up for data stream processing: (1) downloading SEVIRI data from NOAA operational servers, (2) data processing with ACSPO-SEVIRI system, (3) data analysis with web-based QC tools. As of the time of this writing, the continuous inflow of SEVIRI 30-minute FD images has been established in collaboration with the AWG Land Team. McIDAS area files are being downloaded from NOAA operational servers in near-real time, reformatted into hdf4.2 files (similar in their structure to the EUMETSAT L1.5 product), and saved on STAR SAN storage provided by the AWG for shared use between different teams within the AWG. Currently, hdf files from January 2008 to the present have been saved on spinning disk. Three more years of data (2005 to 2007) have been added recently from the University of Wisconsin/CIMMS archives. Case studies processing is done on the SST Team’s Linux computers.

The product file contains up to 32 data layers (Fig. 1), stored in HDF format with internal compression (zip). Average FD product file size is ~450MB. Execution time is ~7min per FD on a DELL PowerEdge 2900 server. Example of the product is shown in Fig. 2 for June 14, 2008, 2:00pm UMT.

4. PRELIMINARY ANALYSES

Analyses of the SEVIRI SST products for this study have been performed offline but these will be fully automated with the web-based QC tools (cf. Fig. 1). Those tools were originally developed for the ACSPO-AVHRR system. Some of them currently process AVHRR data from four platforms (NOAA-16, -17, -18, and MetOp-A) in NRT (Liang et al., 2009; Dash et al., 2009). These tools are currently being adapted to the SEVIRI data. This section quickly illustrates the capabilities of these tools as applied to ACSPO-SEVIRI retrievals for the month of June 2008.

4.1 IMPACT OF ENVIRONMENTAL CONDITIONS

The Single Sensor Error Statistics (SSES) tool analyzes SST retrievals as a function of various environmental conditions, including view/illumination conditions, ambient clouds, water vapor, and wind speed (Xu et al., 2009).

Fig. 3 shows “retrieved – Reynolds” SST as a function of local time. Each point in the graph is an average over one full disk, and solid lines additionally show the result of averaging all 30 days in June, to estimate a “monthly average" diurnal cycle. The absolute values of SST anomalies from regression and physical SSTs may be biased, due to the empirical bias correction applied to both algorithms (see section 3.) However, this bias correction should not affect the amplitude of the diurnal cycle which is ~0.3°C in both SST products.

Fig. 4 shows the time series for the full month of June 2008, each point being a FD mean SST anomaly. The FD average diurnal cycle changes from day to day.

To gain further insight into the mechanisms affecting the diurnal cycle, Fig. 5 plots SST anomaly as a function of wind speed, for midday and midnight. At night, SST is fairly insensitive to wind speed, whereas during daytime, SST changes as a function of wind speed with an amplitude of ~0.7°C. The difference between day and night is largest at low winds, due to the forming of a strong diurnal thermocline. The higher the wind speed, the smaller the diurnal heating.

Fig. 6 further shows that SST depends upon ambient clear-sky conditions during both day and night. The diurnal signal is smallest when ambient cloudiness is high (NAC→0) and largest under clear skies (NAC~400).

4.2. CRTM AND BT SIMULATIONS

The Monitoring IR Clear Sky Radiance over Oceans (MICROS) tool is currently employed in NRT to generate statistics of Model (CRTM) minus Observation (AVHRR) for several NOAA and MetOp platforms http://www.star.nesdis.noaa.gov/sod/sst/micros/ (Liang et al., 2009). These analyses are instrumental for physical SST retrievals, improved cloud mask, and to monitor quality of clear-sky radiances over oceans. Here, the MICROS tool was employed offline to preliminarily test the radiances in the SEVIRI thermal bands.

Fig. 7 plots Model (CRTM) minus Observation (SEVIRI) ("M-O") biases using nighttime data (sun zenith angle > 90°) from one FD image. High M-O biases of ~+0.6K in Ch9 (10.8 μm) and ~+0.3K in Ch10 (12 μm) are consistent with AVHRR biases in similar bands (Liang et al., 2009). They may be due to the CRTM (missing aerosol, using bulk rather than skin SST, and not correcting Reynolds SST for diurnal cycle before inputting to CRTM) or SEVIRI data (which may be subject to residual cloud; cf. Fig. 6). However, the low bias in Ch4 (3.92 μm) is inconsistent with AVHRR analyses. Fig. 8 further confirms that these observations from one FD image remain valid for the full month of June 2008. More analyses are needed to better quantify these preliminary observations, and to resolve the Ch4 anomaly.

4.3. COMPARISON WITH GLOBAL REFERENCE SST FIELDS

The SST Quality Monitor (SQUAM) web-based tool http://www.star.nesdis.noaa.gov/sod/sst/squam/ is currently employed in NRT to generate statistics on the consistency between the AVHRR retrieved SST and multiple reference SST fields (Dash et al., 2009). In this study, the SQUAM tool was run offline to preliminarily test the ACSPO-SEVIRI data for the month of June 2008. Currently used reference fields are listed in Table 2 and include OISST, OISST(A), RTG HR/LR, and OSTIA. Reference data fields will be extended with buoy data in near future.

Fig. 9 shows an example of "Retrieved minus OSTIA" SST histogram. The shape of the histogram is close to Gaussian. FD bias is within ~0.06K and the FD STD is ~0.6K. Note that these analyses were performed in the complete FD domain (SZA, VZA<90°) and no data were withdrawn from the analyses, which may explain the higher than expected STD (recall that AVHHR data show 0.4-0.5K STD wrt OSTIA SST; Dash et al., 2009).

Fig. 10 shows the time series of bias for daytime SEVIRI SST with respect to multiple reference SSTs and Fig. 11 shows the corresponding time series of STDs. Each data point represents the FD average over a 24hr interval. The bias ranges from near 0 to 0.2 K while STD changes from 0.4 to 0.8K depending upon day and reference state, and there is significant variability from day to day. Part of the noise comes from the unconstrained domain SZA, VZA<90°.

5. CONCLUSION AND FUTURE WORK

The ACSPO-SEVIRI end-to-end NRT system has been initially set up and preliminarily evaluated with automated QC tools. Initial results indicate that the system is able to generate the suite of required products. Future work will be aimed at full exploitation of the unique features of the geostationary observations. The ACSPO-SEVIRI system will be optimized, fine-tuned and stress-tested with long time series of SEVIRI data. The following specific tasks will be performed:

- Optimize and validate the CRTM in conjunction with Reynolds SST and NCEP GFS, resolve Ch4 anomaly;
- Optimize Physical and Regression SST algorithms, extensively cross-evaluate the two products, and combine into more accurate Hybrid SST;
- Fully implement and optimize cloud mask;
- Calibrate/Validate SEVIRI SSTs against *in-situ* data;
- Optimize ACSPO processing speed and product volume;
- Analyze diurnal cycle and explore diurnal data compression (using e.g., the principal component analysis)
- Perform long-term analysis of SST with respect to multiple reference SSTs;
- Consider generating higher-level products (L3/L4).

REFERENCES

Le Borgne P., G. Legendre, A. Marsouin, 2006: Operational SST retrieval from MSG/SEVIRI data, EUMETSAT Meteorological Satellite Conference, 12-16 June 2006, Helsinki, Finland.

Dash P., A. Ignatov, Y. Kihai, J. Sapper, 2009: Web-based global quality control and monitoring of NESDIS AVHRR SST products for long term stability and cross-platform consistency in near real-time, AMS conference, Jan 11-15, 2009, Phoenix, AZ (poster JP8.1).

Liang X., A. Ignatov, and Y. Kihai, 2009: Implementation of the Community Radiative Transfer Model (CRTM) in the Advanced Clear-Sky Processor for Oceans (ACSPO) and validation against nighttime radiances, *JGR* (in press).

Liang X., A. Ignatov, Y. Kihai, and F. Xu, 2009: Monitoring of IR Clear-sky Radiances over Oceans for SST (MICROS): Near-Real Time, Web-Based Tool for Monitoring CRTM-AVHRR Biases for Improved Cloud Mask and SST Retrievals, AMS conference, Jan 11-15, 2009, Phoenix, AZ (poster JP5.3).

Merchant C., P. Le Borgne, A. Marsouin, H. Roquet, 2008: Optimal estimation of sea surface temperature from split-window observations, *RSE* (in press).

De Paepe B., Ignatov, A., Dewitte, S., Ipe, A. 2008: Aerosol retrieval over Ocean from SEVIRI for the use in GERB Earth's radiation budget analysis, *RSE*, **112**, 2455-2468.

Petrenko, B., A. Ignatov, Y. Kihai, X. Liang, N. Shabanov, and A. K. Heidinger, 2009: Cloud mask and Quality control for SST within the Advanced Clear Sky Processor for Oceans (ACSPO), AMS conference, Jan 11-15, 2009, Phoenix, AZ (poster JP1.12).

Schmetz J., P. Pili, S. Tjemkes, D. Just, J. Kerkmann, S. Rota, A. Ratier, 2002: An Introduction to Meteosat Second Generation, *BAMS*, **83**, 977-992.

Walton C.C., W.G. Pichel, J.F. Sapper, D.A. May, 2009: The development and operational application of nonlinear algorithms for the measurement of SSTs with the NOAA polar-orbiting environmental satellites. *JGR*, **103**, 27999- 28012.

Xu F., A. Ignatov, and X. Liang, 2009: Towards continuous error characterization in the Advanced Clear-Sky Processor for Oceans (ACSPO) SST, AMS conference, Jan 11-15, 2009, Phoenix, AZ (poster JP1.13).

FTP SOURCES

FTP1 (OISST): ftp.emc.ncep.noaa.gov /cmb/sst/oisst_v2

FTP2 (OISST(A)): eclipse.ncdc.noaa.gov /pub/OI–daily/NetCDF

FTP 3 (RTG SST LR): polar.ncep.noaa.gov /pub/history/sst

FTP4 (RTG SST HR): polar.ncep.noaa.gov /pub/history/sst/ophi

FTP5 (OSTIA): podaac.jpl.nasa.gov /GHRSST/data/L4/GLOB/UKMO/OSTIA

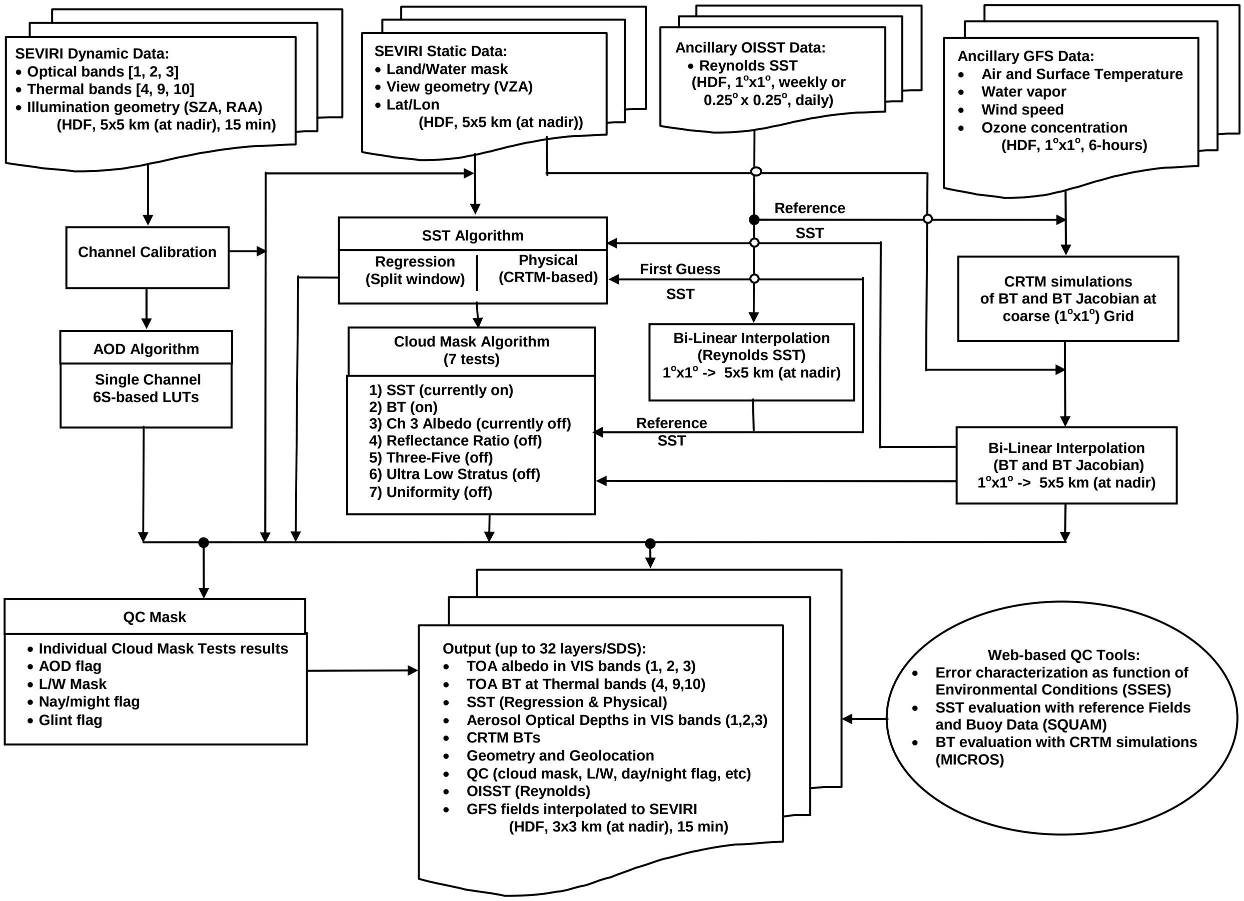

Fig. 1. Flow-chart of the ACSPO-SEVIRI system.

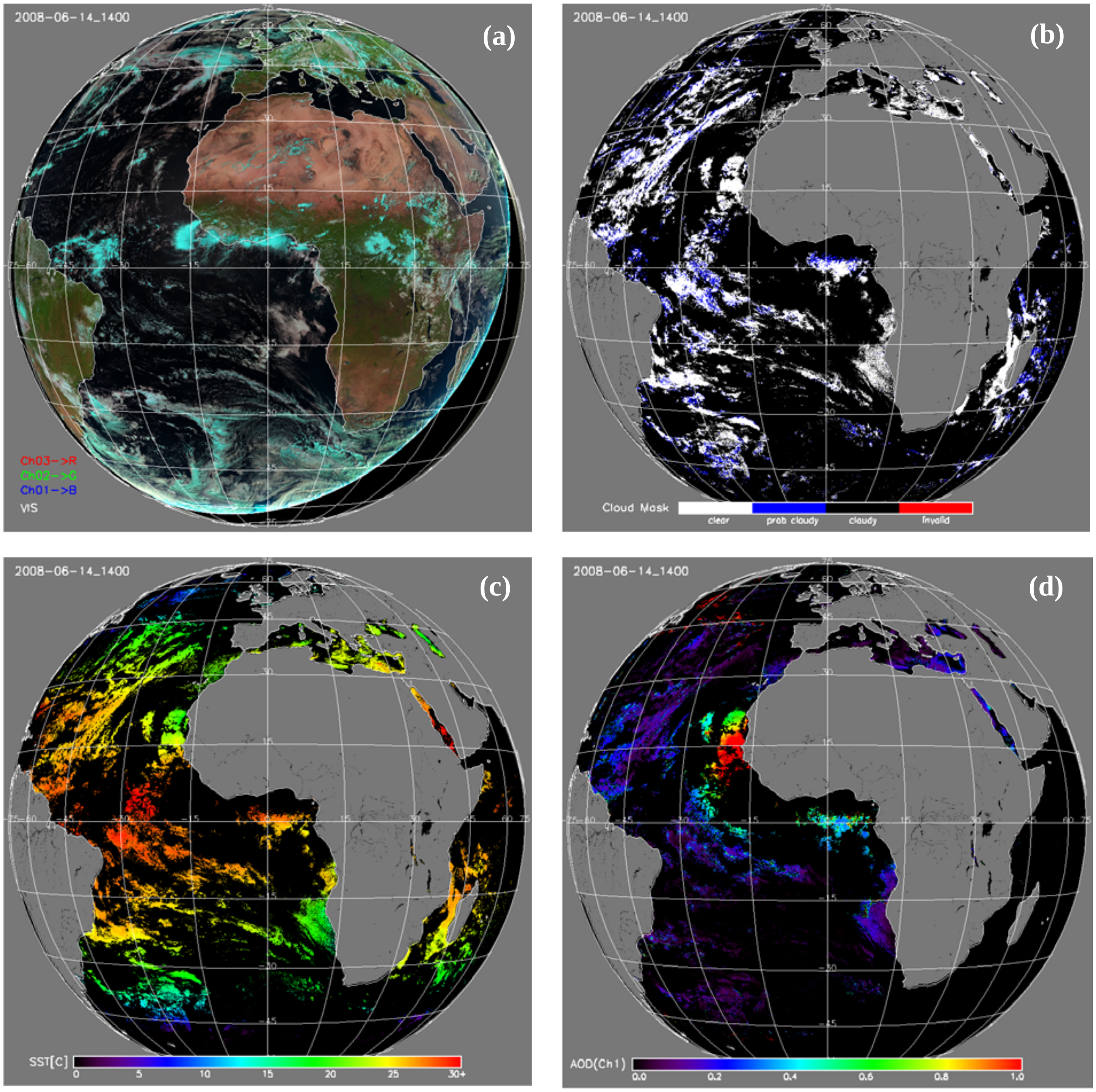

Fig. 2. Example of MSG-2 SEVIRI 15-min FD data for June 14, 2008, 2:00pm UMT, processed by the ACSPO-SEVIRI system. (a) Visible true-color image of Ch1 albedo. Black strip expanding from SE corresponds to night-time; (b) Cloud Mask; (c) physical SST; (d) AOD retrieved from Ch01 using single-channel algorithm (De Paepe et al., 2008).

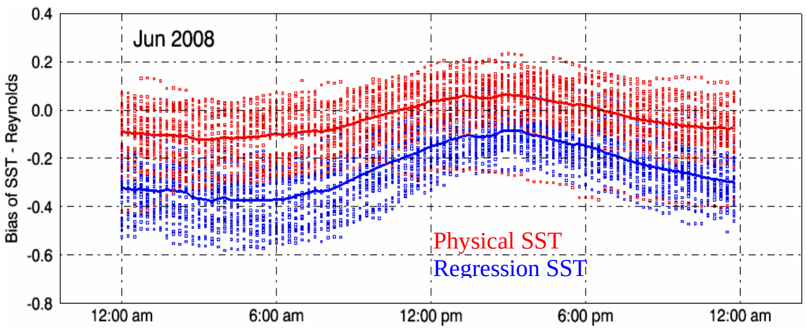

Fig. 3. Solid lines show FD monthly mean diurnal cycles of "Retrieved minus Reynolds SST". Individual data points correspond to different days in June 2008.

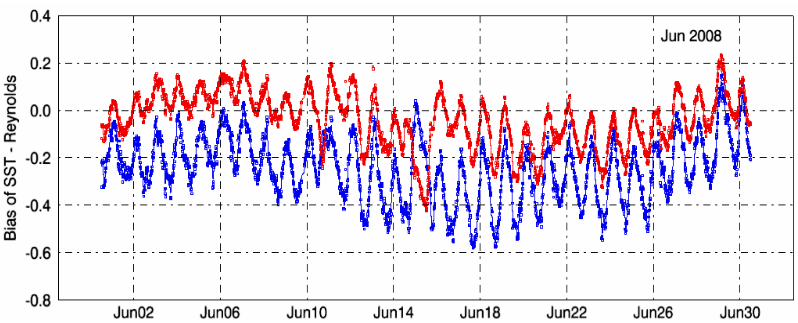

Fig. 4. Time series of "Retrieved minus Reynolds" SST anomalies evaluated over clear sky pixels for June 2008.

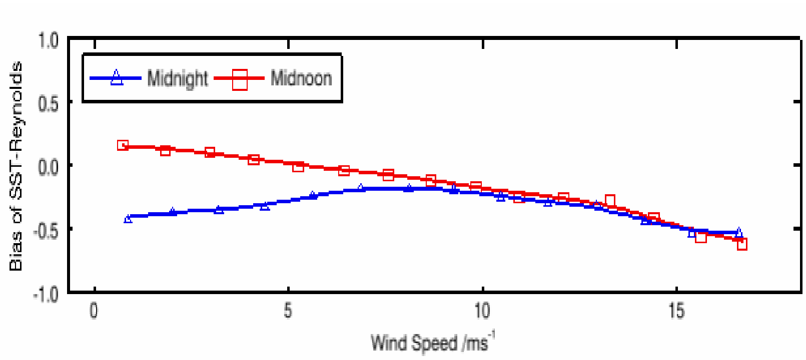

Fig. 5. Physical minus Reynolds SST anomaly as a function of wind speed. FD data from 1-7 June 2008 are binned at V=1 m/s and averaged for 2 hours centered on Midday and Midnight.

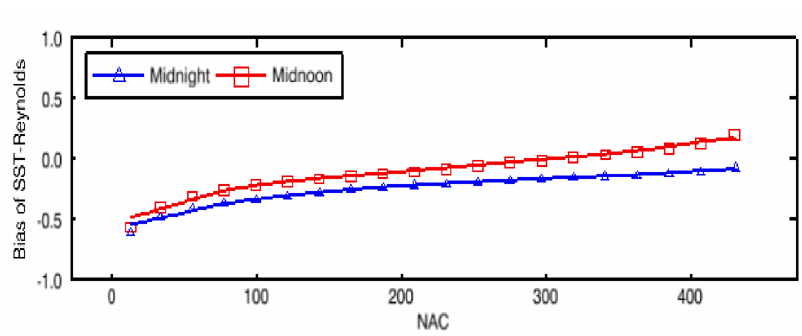

Fig. 6. "Retrieved minus Reynolds" SST anomaly as function of Number of Ambient Clear-Sky pixels (NAC; calculated within 21×21 GAC pixels; Xu et al., 2009). FD data from 1-7 June 2008 are binned at NAC=20 and averaged for 2 hours centered on Midday and Midnight.

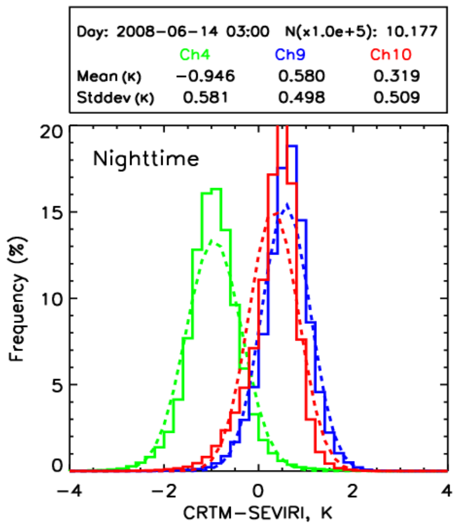

Fig. 7. Nighttime (SZA>90°) "Model minus Observation" biases in SEVIRI Ch4 (3.92 μm), 9 (10.8 μm), and 10 (12 μm) for one FD image taken on 14 June 2008 @ 3:00am. Data shown are for Satellite VZA < 70°.

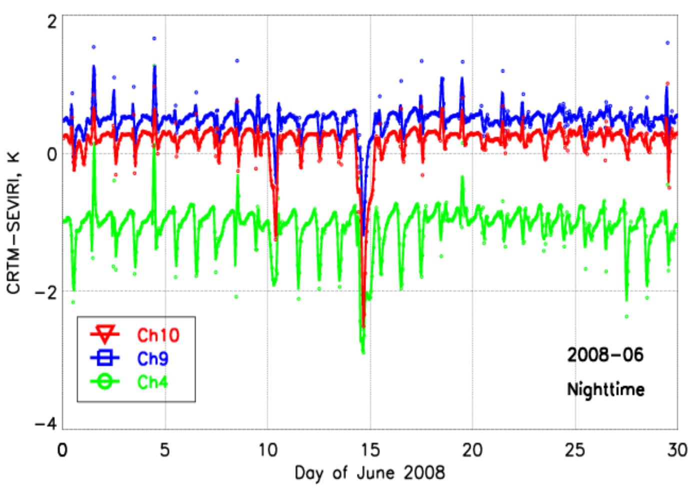

Fig. 8. Time Series of M-O biases in SEVIRI Ch4, 9 and 10 in June 2008. (Nighttime data with SZA>90° and VZA<70°). The root causes of the two drop-out anomalies on 11 and 15 June 2008 are being investigated.

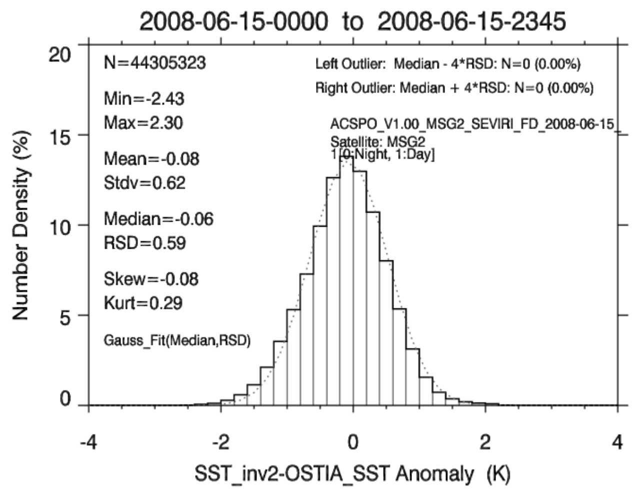

Fig. 9. Example FD histogram of daytime (SZA<90°) SEVIRI SST (physical retrievals) referenced to OSTIA SST for 15 June 2008 @ 23:45UTC. Global statistics of SST anomaly are superimposed. The shape of the histogram is close to Gaussian. The mean bias averaged over the FD is ~-0.06K. The global standard deviation is ~0.62K. (Robust Stdv~0.59K.)

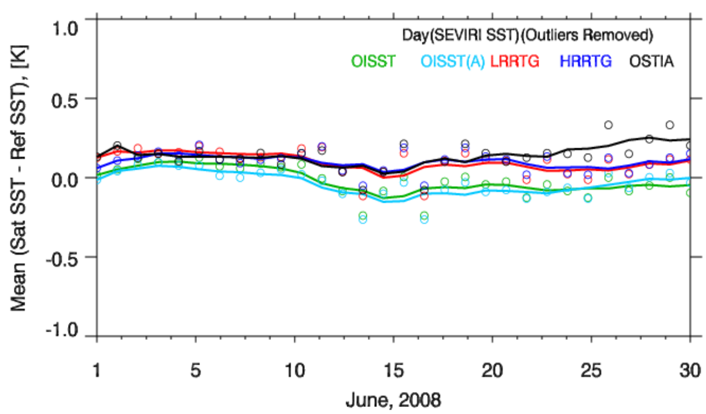

Fig. 10. Time series of bias for daytime (SZA, VZA<90°) SEVIRI SST wrt multiple reference SSTs. Each data point represents FD average over 24hr interval. (Note that the physical SST in this study was tuned against Reynolds SST and therefore bias wrt both OISSTs is smallest whereas wrt OSTIA it is highest ~0.2K).

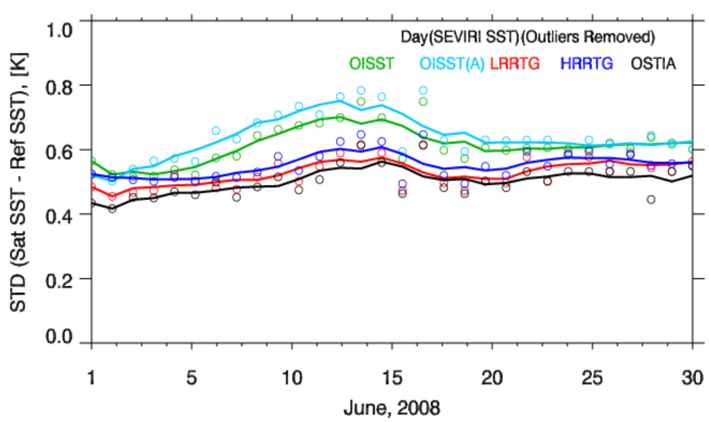

Fig. 11. Time series of STD for daytime SEVIRI SST wrt multiple reference SSTs. Each data point represents STD around mean over FD×24hr. The STD changes from 0.4K to 0.8K depending upon day and reference state, and there is a significant variability from day to day. Part of this noise is deemed to be due to the unconstrained retrieval domain SZA, VZA<90°.